Comparing Treatments for Amblyopia with a Synaptic Plasticity Model

.

Brian S. Blais

10/20/22

These notes are an exploration of the problem of modeling Amblyopia and its various treatments from an approach using synaptic plasticity models. The process will involve constructing a simplified mechanism for the development of amblyopic deficits and subsequentially modeling both monocular and binocular treatment protocols. The goal is to understand the dynamics of the recovery from amblyopic deficits for the different treatment protocols, to compare the effectiveness of each protocol, and to explore their limitations. Ideally we would like to use these models to inform future protocol parameters and perhaps suggest novel treatments for amblyopia.

Table of contents

Preface

These notes are produced with Quarto. (https://quarto.org/docs/books)

Software Installation

The software is Python-based with parts written in Cython.

- Download the Anaconda Distribution of Python: https://www.anaconda.com/products/individual#downl

- Download and extract the *PlasticNet* package at: https://github.com/bblais/Plasticnet/archive/refs/heads
- Run the script `install.py`

Part I

Introduction

1 What is Amblyopia?

Amblyopia is the most common cause of vision loss in children, caused by refractive errors or misalignment of the eyes (Zárate and Tejedor 2007).

- Visual acuity
- Contrast sensitivity
- Color
- Depth (Stereopsis)
- Motion
- Visual fields

1.1 How is it Treated?

The current primary treatment is described in the *Amblyopia Preferred Practice Method* (D. K. Wallace et al. 2018). Treatments are divided into two broad categories, monocular and binocular treatments. Monocular treatments produce a competition between the two eyes by treating only the fellow eye to that the amblyopic eye recovers. Binocular treatments seek to stimulate both eyes in such a way that binocular mechanisms can produce a recovery in the amblyopic eye.

1.1.1 Monocular Treatments

The most common treatment includes

1. the optical correction of significant refractive errors and
2. patching the dominant eye which forces the visual input to come from only the amblyopic eye.

Although patching is the most common method of treatment, other methods are described including pharmacology and technology (Jonathan M. Holmes et al. 2016b; Kelly et al. 2016; Jonathan M. Holmes et al. 2016a; Li et al. 2015; Zárate and Tejedor 2007; Gao et al. 2018; Glaser et al. 2002). These include,

3. Pharmacological treatment with atropine drops in the fellow eye

1.1.2 Binocular Treatments

4. Virtual reality input to both eyes, with contrast modification and/or dichoptic masks

1.2 Mechanisms for Amblyopia

Since the unequal visual input to the brain can cause alterations in the synaptic pathways leading to a disparity in ocular dominance (Birch 2013), it is important to understand the possible synaptic effects amblyopia can produce and how potential treatments will either help or hinder the recovery.

Part II

Methods

In this paper we use a specific model of neural plasticity, the BCM model(Bienenstock, Cooper, and Munro 1982), to describe the dynamics of the recovery from amblyopia under a number of treatment protocols.

2 Natural Image Input Environment

```
%matplotlib inline
from input_environment_defs import *
```

In order to approximate the visual system, we start with the following basic properties of the retina, LGN and cortex. There are approximately 1000 photoreceptors feeding into 1 ganglion cell (Jeon, Strettoi, and Masland 1998; Sterling, Freed, and Smith 1988). The retina/LGN responses show a center-surround organization, but with a center diameter less than 1^o (Hubel 1995)

We use natural scene stimuli for the simulated inputs to the visual system. We start with images taken with a digital camera, with dimensions 1200 pixels by 1600 pixels and 40^o by 60^o real-world angular dimensions (Figure Figure 2.1). Photoreceptors have a logarithmic response to the stimulus, so we apply the natural logarithm to the pixel values. Finally, we model the ganglion responses using a 32x32 pixel center-surround difference-of-Gaussians (DOG) filter to process the images, each pixel representing one photoreceptor (Figure Figure 2.2). The center-surround radius ratio used for the ganglion cell is 1:3, with balanced excitatory and inhibitory regions and normalized Gaussian profiles.

```
# Make the original image files
make_original_image_files()
```

```
fname='asdf/bbsk081604_all.asdf'
image_data=pi5.asdf_load_images(fname)
im=[arr.astype(float)*image_data['im_scale_shift'][0]+
        image_data['im_scale_shift'][1] for arr in image_data['im']]
del image_data
plt.figure(figsize=(16,8))
for i in range(6):
    plt.subplot(2,3,i+1)
    plt.imshow(im[i],cmap=plt.cm.gray)
    plt.axis('off')
```

Figure 2.1: A Small Subset of the Original Natural Images

```
# Make the logged image files

if not os.path.exists('asdf/bbsk081604_all_log2dog.asdf'):
    im=[np.log2(I-I.min()+1) for I in var['im']]
    var_log={'im':im,'im_scale_shift':[1.0,0.0]}
    var_norm=filters.make_norm(var_log)
    var_dog=filters.make_dog(var_norm)
    filters.set_resolution(var_dog,'uint16')
    pi5.asdf_save_images(var_dog,'asdf/bbsk081604_all_log2dog.asdf')
    del var_norm, var_dog, var
```

```
fname='asdf/bbsk081604_all_log2dog.asdf'
image_data=pi5.asdf_load_images(fname)
im=[arr.astype(float)*image_data['im_scale_shift'][0]+
        image_data['im_scale_shift'][1] for arr in image_data['im']]
del image_data
plt.figure(figsize=(16,8))
for i in range(6):
    plt.subplot(2,3,i+1)
    plt.imshow(im[i],cmap=plt.cm.gray)
    plt.axis('off')
```

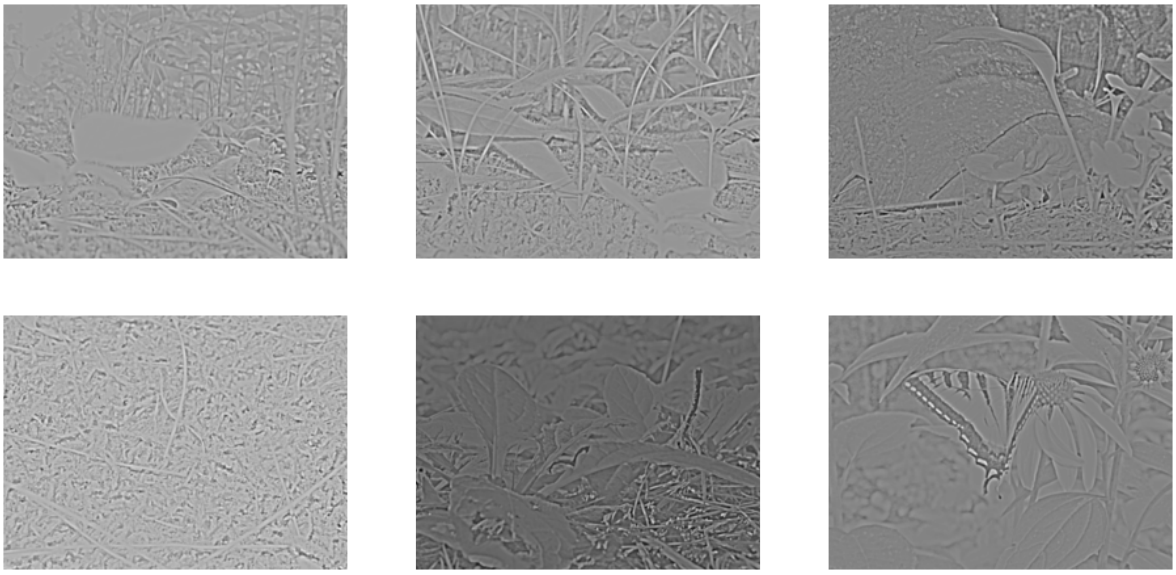

Figure 2.2: A Small Subset of the Natural Images filtered with a base-2 Log function and a difference of Gaussians (DOG)

2.1 Two-eye architecture

Shown in Figure Figure 2.3 is the visual field, approximated here as a two-dimensional projection, to left and right retinal cells. These left and right retinal cells project to the left and right LGN cells, respectively, and finally to a single cortical cell. The LGN is assumed to be a simple relay, and does not modify the incoming retinal activity. It is important to understand that the model we are pursuing here is a *single cortical cell* which receives input from both eyes. We will encounter some limitations to this model which may necessitate exploring multi-neuron systems.

In the model, normal development is simulated with identical image patches presented to both eyes combined with small independent noise in each eye. The random noise is generated from a zero-mean normal distribution of a particular variance, representing the natural variation in responses of LGN neurons. Practically, the independent random noise added to each of the two-eye channels avoids the artificial situation of having mathematically identical inputs in the channels. The development of the deficit and the subsequent treatment protocols are modeled with added preprocessing to these image patches, described below in Sections **?@sec-models-of-deficit** and Chapter 5.

For all of the simulations we use a 19x19 receptive field, which is a compromise between speed of simulation and the limits of spatial discretization. We perform at least 20 independent simulations for each condition to address variation in the results.

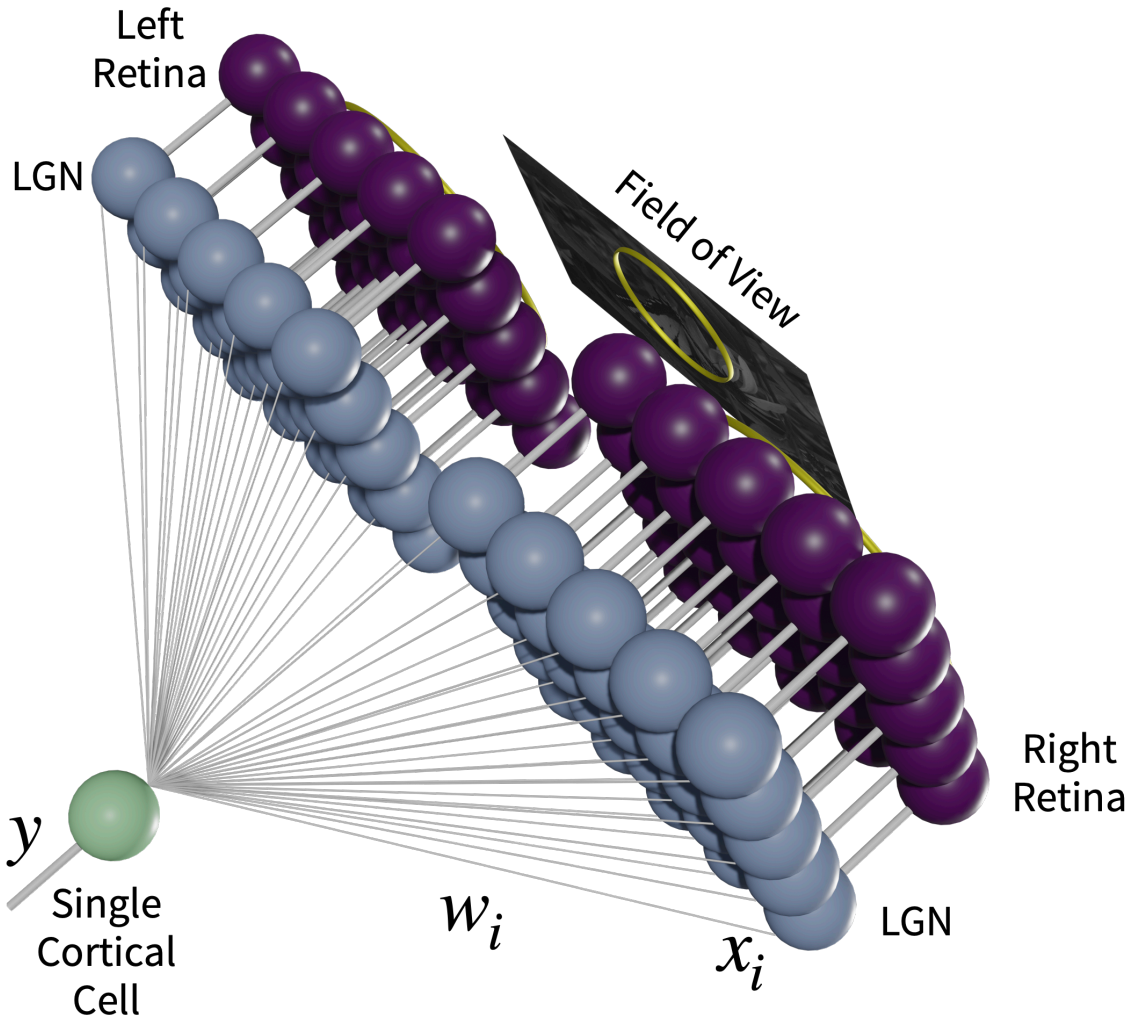

Figure 2.3: Two-eye Architecture.

```
sim,X=get_input_patch_examples(blur=-1)
ims=inputs_to_images(X,buffer=2)
figure(figsize=(20,6))
for i in range(24):
    im=ims[i]
    subplot(4,6,i+1)
    imshow(im,cmap=plt.cm.gray)
    axis('off')
```

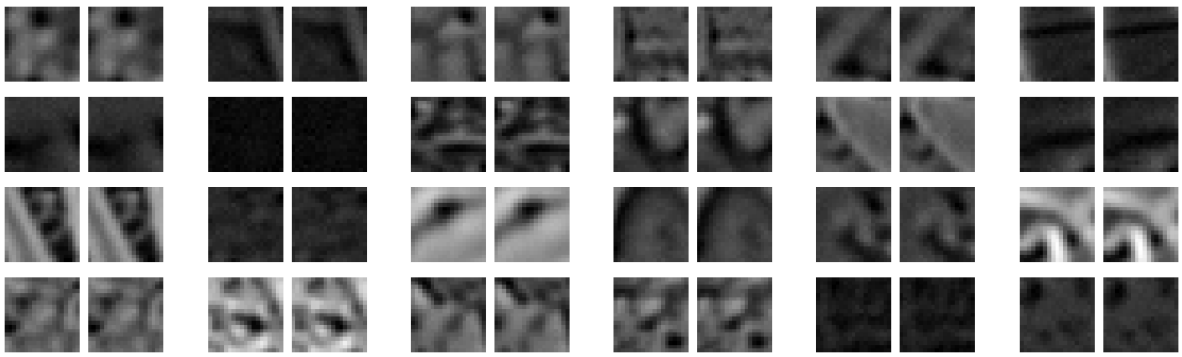

Figure 2.4: A sample of 24 input patches from a normal visual environment. The left- and right-eye inputs are shown in pairs.

3 Synaptic Modification

```
%matplotlib inline
from input_environment_defs import *
from deficit_defs import Results
```

3.1 The BCM Learning Rule

We use a single neuron and the parabolic form of the BCM(Bienenstock, Cooper, and Munro 1982; Brian S. Blais et al. 2008) learning rule for all of the simulations, where the synaptic modification depends on the postsynaptic activity, y, in the following way for a single neuron

$$y = \sigma\left(\sum_i x_i w_i\right)$$
$$\frac{dw_i}{dt} = \eta y(y - \theta_M)x_i$$
$$\frac{d\theta_M}{dt} = (y^2 - \theta_M)/\tau$$

where is x_i is the ith presynaptic input, w_i is the ith synaptic weight, and y is the postsynaptic output activity. The constant, η, refers to the learning rate and the constant, τ, is what we call the memory-constant and is related to the speed of the sliding threshold. The transfer function, $\sigma(\cdot)$, places minimum and maximum responses given a set of inputs and weights.

```
y=np.linspace(-5,20,100)
 _M=8
 =y*(y- _M)

plot(y, ,'b-')

yl=gca().get_ylim()
plot([0,0],yl,'k--')
gca().set_ylim(yl)
```

```
xl=gca().get_xlim()
plot(xl,[0,0],'k--')
gca().set_xlim(xl)

plt.text( _M,30,r'$\theta_M$',ha='center',va='center')
plt.arrow( _M+1,30,5,0,color='r',length_includes_head=True,
              head_width=5, head_length=.6,lw=2)
plt.arrow( _M-1,30,-5,0,color='r',length_includes_head=True,
              head_width=5, head_length=.6,lw=2)
plot([ _M, _M],[-10,10],'r-',lw=2)
xlabel('Neuron output ($y$)')
ylabel('Change in the synaptic weight ($dw/dt$)');
```

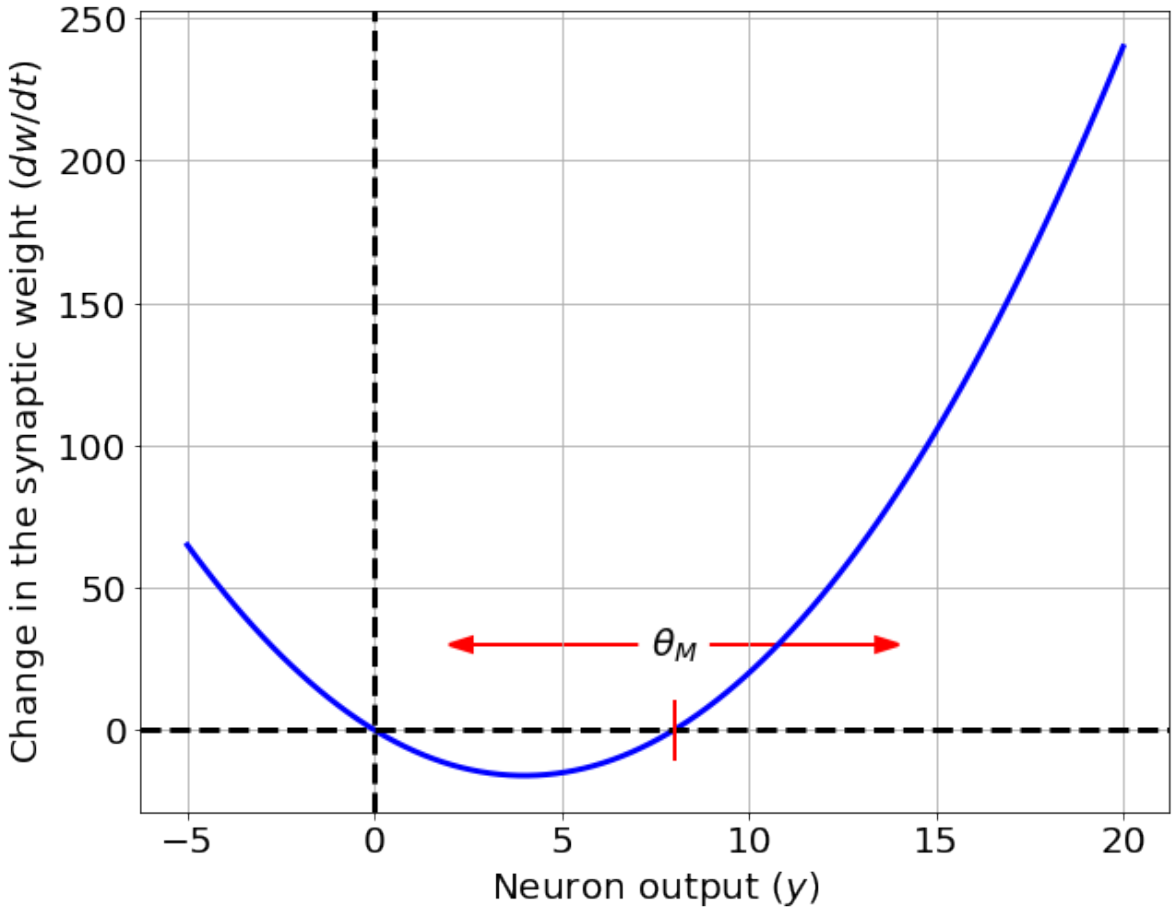

Figure 3.1: The BCM synaptic modification function. Units are arbitrary.

The results are extremely robust to values of η and τ , which are generally chosen for practical, rather than theoretical, considerations. Each of these constants is related to the time-step for the simulations, but given the phenomenological nature of the BCM theory it is beyond the scope of this paper to make detailed comparisons between simulation time and real-time. Further, the fact that τ can be changed within a factor of 100 with no noticeable effect, the experiments presented here cannot be used address the time-scales of the molecular mechanisms underlying synaptic modification. Whenever we refer to real-time units for a simulation, we approximate a single simulation iteration as 1 iteration = 0.2 seconds(Brian S. Blais 1998).

In the BCM learning rule, weights decrease if y is less than the modification threshold,θ_M , and increase if y is greater than the modification threshold. To stabilize learning, the modification threshold "slides" as a super-linear function of the output. The output, y , is related to the product of the inputs and the weights via a sigmoidal function, $\sigma(\cdot)$, which places constraints on the values of the output, keeping it in the range -1 and 50. The interpretation of negative values is consistent with previous work(B. S. Blais et al. 1998), where the activity values are measured relative to spontaneous activity. Thus, negative values are interpreted as activity below spontaneous. We continue this usage, in order to more easily compare with previous simulations. The role of the spontaneous level for the simulations in the natural image environment is discussed elsewhere(B. S. Blais et al. 1998).

3.2 Simulation

The synaptic weights, and the modification threshold, are set to small random initial values at the beginning of a simulation. At each iteration, an input patch is generated as described above depending on the procedure being simulated and then presented to the neuron. After each input patch is presented, the weights are modified using the output of the neuron, the input values and the current value of the modification threshold. In an input environment composed of patches taken from natural images, with equal patches presented to the left- and right-eyes as shown in Figure 2.4, this process orientation selective and fully binocular cells(B. S. Blais et al. 1998). We then present test stimulus made from sine-gratings with 24 orientations, 20 spatial frequencies, and optimized over phase. Applying any of the blur filters to the sine gratings does not quantitatively change the result.

```
fname=pi5.filtered_images('asdf/bbsk081604_all_log2dog.asdf')

pre1=pn.neurons.natural_images(fname,
                               rf_size=19,verbose=False)

pre2=pn.neurons.natural_images(fname,rf_size=19,
                            other_channel=pre1,
                            verbose=False)
```

```
pre1+=pn.neurons.process.add_noise_normal(0,0.5) # a little noise
pre2+=pn.neurons.process.add_noise_normal(0,0.5) # a little noise


pre=pre1+pre2

number_of_neurons=5
post=pn.neurons.linear_neuron(number_of_neurons)
post+=pn.neurons.process.sigmoid(0,50)

c=pn.connections.BCM(pre,post,[-.01,.01],[.1,.2])
c+=pn.connections.process.orthogonalization(10*minute)
c.eta=2e-6
c.tau=15*minute

sim=pn.simulation(4*day)
sim.dt=200*ms

save_interval=30*minute
sim.monitor(post,['output'],save_interval)
sim.monitor(c,['weights','theta'],save_interval)

sim+=pn.grating_response()

pn.run_sim(sim,[pre,post],[c],display_hash=True,print_time=True)
pn.save('sims/nr.asdf',sim,[pre,post],[c])
R=Results('sims/nr.asdf')
```

```
def argmax_rc(X):
    """Return the row and col of the maximum value"""
    r,c=np.unravel_index(np.argmax(X), X.shape)
    return r,c
```

```
figure(figsize=(4,10))
R.plot_rf()

figure(figsize=(10,8))
plot(R.t/hour,R. ,label=[f'Neuron {i}' for i in [0,1,2,3,4]])
ylabel(r'$\theta_M$')
xlabel('Time (hours)')
```

```
legend();

figure(figsize=(10,8))
t,y=R.all_responses[0]
for neuron in range(5):
    subplot(2,1,1)
    y_left=y[:,:,0,neuron,-1]
    y_right=y[:,:,1,neuron,-1]

    r,c=argmax_rc(y_left)
    tuning_curve=y_left[r,:]
    plot(R.theta_mat,tuning_curve,'-o')
    plt.title('Left-eye Responses')
    ylabel('Response')
    gca().set_xticklabels([])

    subplot(2,1,2)
    r,c=argmax_rc(y_right)
    tuning_curve=y_right[r,:]
    plot(R.theta_mat,tuning_curve,'-s')
    plt.title('Right-eye Responses')
    ylabel('Response')
    xlabel('Angle of Stimulus')
```

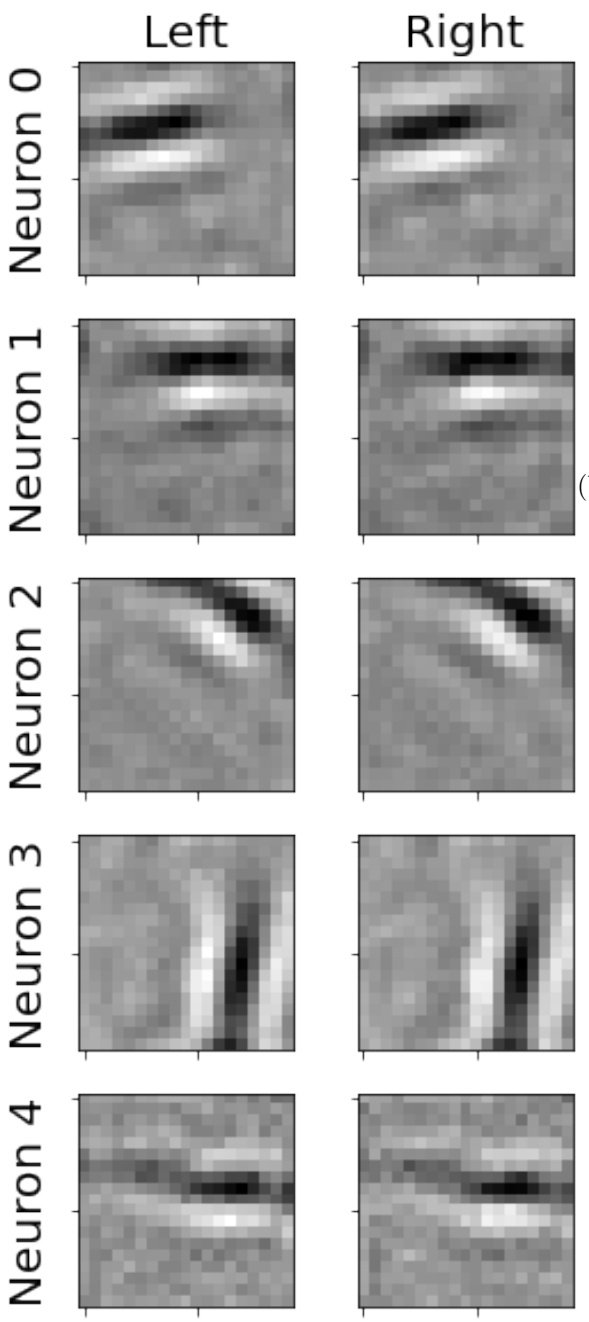

(a) Synaptic weights where black denotes weak weights and white denotes strone weights. A clear preference for oriented stimuli can be seen.

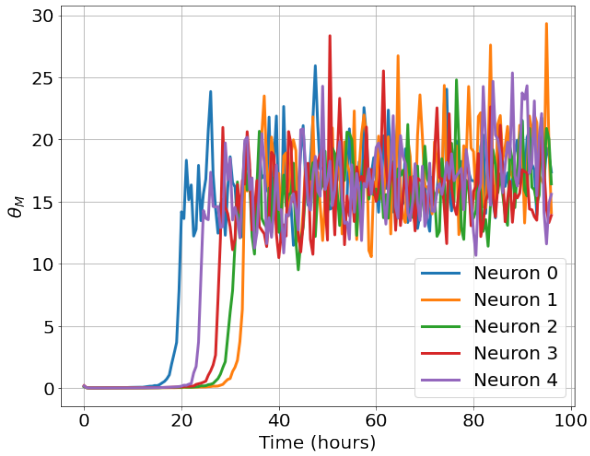

(b) BCM modification threshold over time. The value converges to nearly the same level for all neurons.

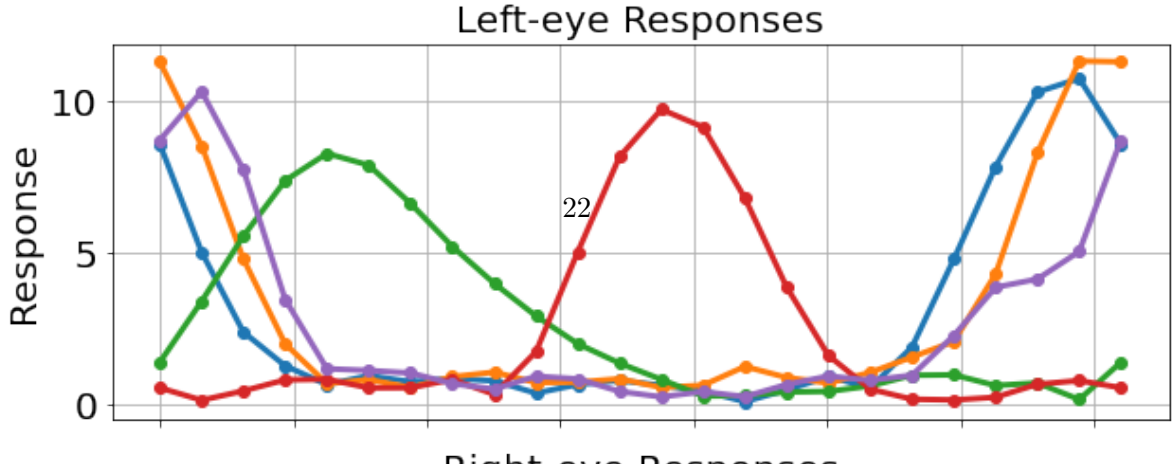

4 Models of Development of Amblyopia

```
%matplotlib inline
from input_environment_defs import *
```

Amblyopia is a reduction of the best-corrected visual acuity (BCVA) with an otherwise normal eye and has many causes(D. K. Wallace et al. 2018). Two of the most common forms of amblyopia are strabismic and anisometropic amblyiopia. Strabismic amblyopia occurs when the inputs from each eye do not converge and the fixating eye becomes dominant over a non-fixating eye. Refractive amblyopia occurs with untreated unilateral refractive errors, one kind being anisometropic amblyopia where unequal refractive power in each eye leads the retinal image from the amblyopic eye to be blurred relative to the fellow eye. Both of these processes lead to synaptic plasticity adjustments and interocular competition, enhancing the initial deficit.

In this work we use a model of the amblyopic deficit caused by two mechanisms. The first is a blurring of the amblyopic eye inputs, representing refractive amblyopia. The second is eye-jitter, representing one source of strabismic amblyopia. We can explore these mechanisms independently and in conjunction to see how they respond differentially to the various treatments.

4.1 Refractive amblyopia

The amblyopic eye is presented with image patches that have been *blurred* with a normalized Gaussian filter applied to the images with a specified width. The larger the width the blurrier the resulting filtered image.

```
sim,X=get_input_patch_examples(blur=2.5)
ims=inputs_to_images(X,buffer=2)
figure(figsize=(20,6))
for i in range(24):
    im=ims[i]
    subplot(4,6,i+1)
    imshow(im,cmap=plt.cm.gray)
```

```
    axis('off')
```

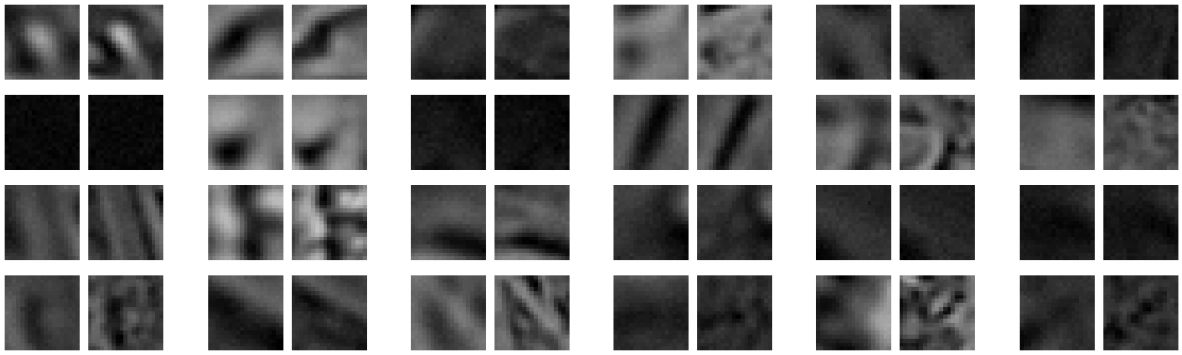

Figure 4.1: A sample of 24 input patches from a refractive amblyopic environment. The amblyopic (blurred) input is the square on the left-hand side of each pair.

4.2 Strabismic amblyopia

Strabismic inputs are modeled by changing the center of the left- and right-input patches in a systematic way, with a set mean offset and a standard deviation per input patch generated. In this way we can model completely overlapping (i.e. normal) inputs, completely non-overlapping (i.e. extreme strabismus), and any amount of overlap in between. Some examples are shown in Figure 4.2 with the offset locations shown in Figure 4.3.

```
mu_r,mu_c=2,10
sigma_r,sigma_c=1,2

sim,X=get_input_patch_examples_with_jitter(blur=-1,mu_r=mu_r,mu_c=mu_c,sigma_r=sigma_r,sig
ims=inputs_to_images(X,buffer=2)
figure(figsize=(20,6))
for i in range(24):
    im=ims[i]
    subplot(4,6,i+1)
    imshow(im,cmap=plt.cm.gray)
    axis('off')
```

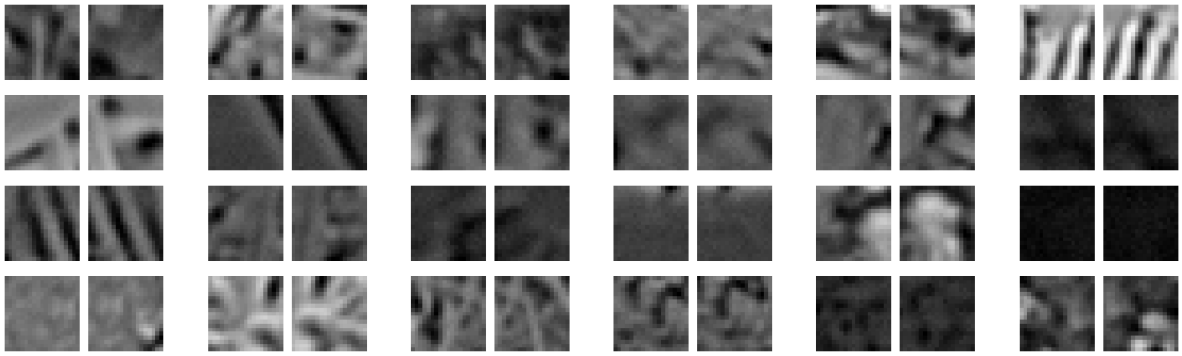

Figure 4.2: A sample of 24 input patches from a strabismic visual environment achieved through random jitter of the amblyopic (left) eye.

```
import matplotlib.patches as patches
ca=sim.monitors['ca'].array()
ra=sim.monitors['ra'].array()
c=sim.monitors['c'].array()
r=sim.monitors['r'].array()

ca_1=sim.monitors['ca_1'].array()
ra_1=sim.monitors['ra_1'].array()
c_1=sim.monitors['c_1'].array()
r_1=sim.monitors['r_1'].array()

figure(figsize=(11,9))
plot(ca-c,-(ra-r),'bo',label='Left')

plot(ca_1-c_1,-(ra_1-r_1),'ro',label='Right')
rect = patches.Rectangle((-19/2, -19/2), 19, 19, linewidth=1, edgecolor='b',lw=2, facecolo
gca().add_patch(rect)
rect = patches.Rectangle((-19/2+mu_c, -19/2-mu_r), 19, 19, linewidth=1, edgecolor='r', lw=
gca().add_patch(rect)
axis('equal');

xlabel('Horizontal Visual Field Location (pixels)')
ylabel('Vertical Visual Field Location (pixels)');
legend();
```

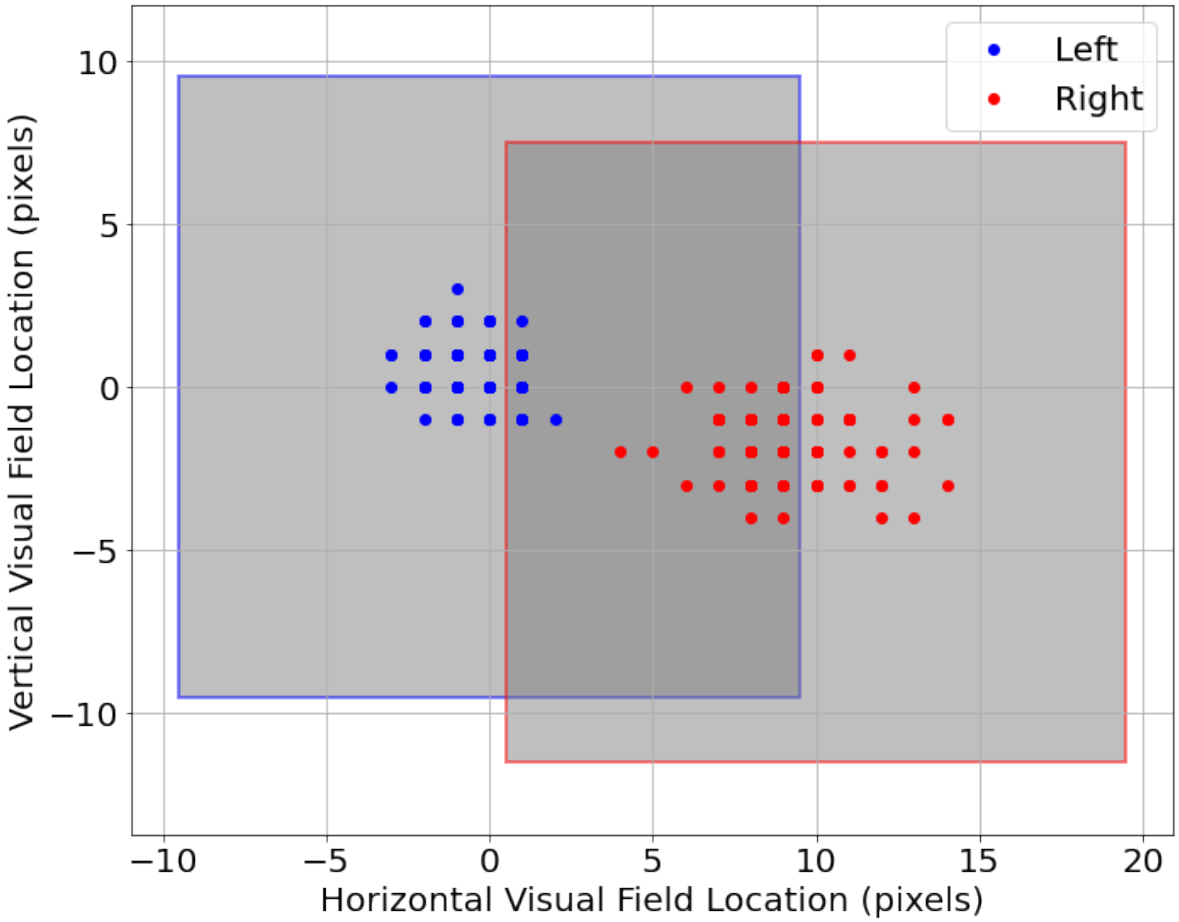

Figure 4.3: Locations of the center of the left- and right-field of view receptive fields, jittered randomly with set mean and standard deviation. The average receptive fields are shown as gray squares.

5 Models of Treatments for Amblyopia

```
%matplotlib inline
import matplotlib.pyplot as plt
import numpy as np
import plasticnet as pn
import process_images_hdf5 as pi5
from deficit_defs import patch_treatment

from matplotlib.pyplot import figure,xlabel,ylabel,legend,gca,plot,subplot,imshow,axis
```

To model the fix to the refractive imbalance we follow the deficit simulation with an input environment that is rebalanced, both eyes receiving nearly identical input patches (Figure 2.4). This process is a model of the application of refractive correction. Although both eyes receive nearly identical input patches, we add independent Gaussian noise to each input channel to represent the natural variation in the activity in each eye. In addition, in those cases where use employ strabismic amblyopia, the inter-eye jitter is not corrected with the refractive correction.

```
def inputs_to_images(X,buffer=5):
    ims=[]
    vmin=X.min()
    vmax=X.max()

    rf_size=int(np.sqrt(X.shape[1]/2))

    for xx in X:
        xx1=xx[:rf_size*rf_size].reshape(rf_size,rf_size)
        xx2=xx[rf_size*rf_size:].reshape(rf_size,rf_size)
        im=np.concatenate((xx1,np.ones((rf_size,buffer))*vmax,xx2),axis=1)
        ims.append(im)

    return ims

def get_input_patch_examples_treatment():
```

```
    seq=pn.Sequence()
    seq+=patch_treatment(patch_noise=0.5,
                total_time=1000,number_of_neurons=1,
                eta=1e-6,
                save_interval=1)
    sim=seq.sims[0]
    pre=seq.neurons[0][0][0]
    sim.monitor(pre,['output'],1)

    seq.run(display_hash=False,print_time=True)
    m=sim.monitors['output']
    t,X=m.arrays()

    return sim,X

sim,X=get_input_patch_examples_treatment()
```

```
    seq=pn.Sequence()
    seq+=patch_treatment(patch_noise=0.5,
                total_time=100,number_of_neurons=1,
                eta=1e-6,
                save_interval=1)
    sim=seq.sims[0]
    pre=seq.neurons[0][0][0]
```

```
Using cache_images_de75a60123a7c262a30ea675be766aff.asdf from cache.
```

```
seq.neurons[0][0][0]
```

```
<plasticnet.neurons.pattern_neuron.natural_images at 0x7fa070153e50>
```

```
X
```

```
array([-0.        , -0.        , -0.        , ..., -0.        ,
       -0.        ,  0.04363927])
```

```
m=sim.monitors['output']
t,X=m.arrays()
```

5.1 Patch treatment

The typical patch treatment is done by depriving the strong-eye of input with an eye-patch. In the model this is equivalent to presenting the strong-eye with random noise instead of the natural image input. Competition between the left- and right-channels drives the recovery, and is produced from the difference between *structured* input into the weak-eye and the *unstructured* (i.e. noise) input into the strong eye. It is not driven by a reduction in input activity.

5.2 Contrast modification

A binocular approach to treatment can be produced with contrast reduction of the non-deprived channel relative to the deprived channel. Experimentally this can be accomplished with VR headsets(Xiao et al. 2020). In the model we implement this by down-scaling the normal, unblurred channel with a simple scalar multiplier applied to each pixel (Figure 4 D). The contrast difference sets up competition between the two channels with the advantage given to the weak-eye channel.

5.3 Dichoptic Mask

On top of the contrast modification, we can include the application of the dichoptic mask (Figure (**fig:input?**) E). In this method, each eye receives a version of the input images filtered through independent masks in each channel, resulting in a mostly-independent pattern in each channel.
It has been observed that contrast modification combined with dichoptic masks can be an effective treatment for amblyopia(**xiao2021randomized?**). The motivation behind the application of the mask filter is that the neural system must use both channels to reconstruct the full image and thus may lead to enhanced recovery.

The dichoptic masks are constructed with the following procedure. A blank image (i.e. all zeros) is made to which is added 15 randomly sized circles with values equal to 1 (Figure (**fig:dichopic_blob?**)). These images are then smoothed with a Gaussian filter of a given width, f. This width is a parameter we can vary to change the overlap between the left- and right-eye images. A high value of f compared with the size of the receptive field, e.g. $f = 90$, yields a high overlap between the patterns in the weak- and strong-eye inputs (Figure (**fig:dichopic_filter_size?**)). Likewise, a small value of f, e.g. $f = 10$, the eye inputs are

nearly independent – the patterned activity falling mostly on one of the eyes and not much to both. Finally, the smoothed images are scaled to have values from a minimum of 0 to a maximum of 1. This image-mask we will call A, and is the left-eye mask whereas the right-eye mask, F, is the inverse of the left-eye mask, $F \equiv 1 - A$. The mask is applied to an image by multiplying the left- and right-eye images by the left- and right-eye masks, respectively, resulting in a pair of images which have no overlap at the peaks of each mask, and nearly equal overlap in the areas of the images where the masks are near 0.5 (Figure (**fig:dichopic_filter_image?**)).

5.4 Atropine treatment

In the atropine treatment for amblyopia(Glaser et al. 2002), eye-drops of atropine are applied to the strong-eye resulting in blurred vision in that eye. Here we use the same blurred filter used to obtain the deficit (possibly with a different width) applied to the strong eye (Figure (**fig:input?**) F). The difference in sharpness between the strong-eye inputs and the weak-eye inputs sets up competition between the two channels with the advantage given to the weak-eye.

6 Ocular Dominance Index

Simulations are ended when selectivity has been achieved and the responses are stable. From the maximal responses of each eye, R_{left} and R_{right}, individually, we can calculate the ocular dominance index as

$$\text{ODI} \equiv \frac{R_{\text{right}} - R_{\text{left}}}{R_{\text{right}} + R_{\text{left}}}$$

The ocular dominance index (ODI) has a value of ODI ≈ 1 when stimulus to the right-eye (typically the strong eye in the simulations, by convention) yields a maximum neuronal response with little or no contribution from the left-eye. Likewise, an ocular dominance index (ODI) has a value of ODI ≈ -1 when stimulus to the left-eye (typically the weak eye, by convention) yields a maximum neuronal response with little or no contribution from the right-eye. A value of ODI ≈ 0 represents a purely binocular cell, responding equally to stimulus in either eye.

> **!** Important
>
> - do an orientation tuning index
> - do a spatial frequency tuning index

Part III

Results

Deficit and Measuring the Effectiveness of a Treatment

Figure (**fig:y_vs_t_fix_n0?**) shows the maximum response to oriented stimuli for $n = 20$ neurons versus time. The first 8 days of simulated time define the *deficit* period, where the neurons start in a naïve state with random synaptic weights, and are presented with natural image input blurred in the weak-eye channel as in Section (**sec:methods?**). Following the deficit, the simulation proceeds into the *fix* period, where the balanced natural image input is restored. This transition is marked with a red line in Figure (**fig:y_vs_t_fix_n0?**). We can see only a modest improvement in the deprived-eye responses to the *fix* treatment. This treatment depends on the noise level presented to the open eye. In Figure (**fig:y_vs_t_fix_n0?**), that noise level is $\sigma_n = 0$ whereas in Figure (**fig:y_vs_t_fix_n1?**) the noise level is $\sigma_n = 1$. Increasing the open-eye noise results in an improved recovery from the deficit.

Figure (**fig:ODI_vs_t_fix_n1?**) shows a measurement of this recovery, using the oculur dominance index described in Section (**sec:ocular-dominance-index?**). Balance responses result in an ODI = 0. As the deficit is increased, so the ODI increases toward 1. After the fix, with high levels of open-eye noise, the neurons nearly all recover from much of their initial deficit – the ODI nearly returns to ODI = 0. A simple measure of the effectiveness of the treatment is the *rate* of the recovery of the ODI:

$$\text{recovery rate} = \frac{ODI_{\text{deficit}} - ODI_{\text{treatment}}}{\text{duration of treatment}}$$

Recovery using glasses

The "fix" treatment described in Section (**sec:models-of-development-and-treatment-of-amblyopia?**) and Section (**sec:deficit-and-measuring-the-effectiveness-of-a-treatment?**) depends on the noise level in the open eye. Figure (**fig:dODI_fix_vs_noise?**) shows the rate of recovery as a function of this noise. For low-noise, there is very little improvement. For large noise, $\sigma_n = 1$, the rate achieves 0.14 [ODI/day]. This measure lets us compare different treatments, and determine which are the most effective under the model assumptions. Because the experimental observation is that glasses alone are only able to fully restore vision in 27% of amblyopia cases(D. Wallace et al. 2006), the other simulations use an open-eye noise value of $\sigma_n = 0.1$.

Patch Treatment

As shown in (**sec:results?**), increased *unstructured* input into the previously dominant eye increases the rate of recovery. This is a general property of the BCM learning rule and has been explored elsewhere(B. Blais, Shouval, and Cooper 1999).

Figure (**fig:dODI_patch_vs_noise?**) shows the effect of the patch treatment as a function of the closed-eye noise. For noise levels above $\sigma_n \sim 0.4$ the patch treatment is more effective than recovery with glasses alone. There is the danger of the patch treatment and some other treatments (see below) of causing reverse amblyopia, producing a deficit in the previously stronger eye. This will be dependent on the magnitude of the initial deficit and the amount of time for the treatment. Because the BCM learning rule works by the competition between patterns, there is no danger of causing reverse amblyopia with the fix with glasses, but there is that danger in any treatment that has an asymmetry between the strong and weak eye, favoring the weak eye, as most treatments have.

#todo - [ ] example of reverse amblyopia

Atropine Treatment

Figure (**fig:dODI_atropine_vs_blur?**) shows the recovery rates under the atropine treatment, where the strong eye is presented with a blurred, noisy version of the natural input. Like the patch treatment, the effect is increased with increasing noise level due to the competition between patterns. When the blur filter is very small, the strong-eye inputs are nearly the same as the weak-eye inputs, yielding a result much like the glasses fix. When the blur filter is larger, the atropine treatment becomes comparable to the patch treatment. The blurred inputs are no better than the patch treatment, which has only the noise input.

Contrast Modification and Dichoptic Masks

Figure (**fig:dODI_constrast?**) shows the recovery rates under a binocular treatment which only involves contrast modification, where the contrast for the strong-eye is adjusted relative to the weak eye. A contrast level of 1 is normal equal-eye vision. A contrast level of 0 means that the strong-eye input is shut off entirely. We see an increased rate of recovery with a smaller contrast value, or a larger difference between the strong- and weak-eye inputs. The rate does not compare to the rate of the patch treatment, because while there is a larger difference between the strong- and weak-eye inputs for lower contrast value, the rate of change of the strong-eye weights is decreased. The patch and atropine treatments result in more competition between patterns, resulting in faster recovery times.

#todo - [ ] discuss optimal contrast level

Figure (**fig:dODI_constrast_mask?**) shows the recovery rates under a binocular treatment which includes both contrast modification and dichoptic masks. The effect of the mask is diminished as the mask filter size increases, which is expected because a larger filter size results in more overlap in the strong- and weak-eye inputs and thus less competition. Interestingly, the mask enhances the effect of contrast on the recovery rates in two ways. For low contrast value

(i.e. strong- and weak-eye inputs are more different) the mask increases the recovery rate and can reach rates comparable or exceeding patch treatment. For extremely low contrast values, where nearly all of the input is coming in from the weak eye, there is possibility of causing reverse amblyopia. For high contrast value (i.e. strong- and weak-eye inputs are nearly the same), the masks not only make the recovery slower, but can even enhance the amblyopia.

7

8

Part IV

Conclusions

#todo - [ ] discuss conclusions > This section actually seems a bit superfluous right now, I wonder if we don't need to try and link the ocular dominance measures with visual acuity > > Instead, we could focus the conclusion on linking the directional conclusions with ODI/day to the existing experimental literature, and making recommendations for future amblyopia treatment studies. Thoughts?

Now that we have a system of simulation environments to explore, we can compare to experimentally observed rates of recovery. From (Glaser et al. 2002) we have results from several visual protocols.

1. Only those patients are included if they had their *refractive error corrected for at least 4 weeks*
2. In the patching group most patients received *no more than 6-8 hours of patching per day*
3. The resulting improvement in the visual acuity (measured in lines) is given here:

Time	Patch [lines]	Atropine [lines]
5 weeks	$+2.22 \pm 0.2$	$+1.37 \pm 0.2$
16 weeks	$+2.94 \pm 0.2$	$+2.42 \pm 0.2$
24 weeks	$+3.16 \pm 0.2$	$+2.84 \pm 0.2$

This small amount of data lets us estimate the relative rates of improvement from the treatments. Since the patch treatment is only about 1/3 day, the total time for treatment would be 19weeks $\times \frac{7\text{day}}{1\text{week}} \times 1/3 = 44\text{day}$ For patch treatment with the above data we have a rate of about 0.94lines/44day = 0.021lines/day. Likewise, for atropine, we have a rate of about 1.47lines/133day = 0.011lines/day. So the patch treatment is approximately twice as fast as the atropine. Looking at Figure (**fig:dODI_atropine_vs_blur?**) we see that this can put a rough constraint on the parameters. For a closed-eye noise for the patch treatment of $\sigma_n = 0.8$ (recovery rate ODI/day ~ 0.2), the atropine treatment must have a lower noise level – we can look at the atropine parameters which yield recover rates ODI/day ~ 0.1). For little blur, we need a noise level of around $\sigma_n = 0.6$, but if the atropine produces a significant blur, then the noise level of those inputs must be much lower – well below $\sigma_n = 0.3$ for blur filter size 6.0, for example.

This noise level for atropine is entirely consistent with the same open-eye noise level with the glasses "fix" discussed earlier. Here we have an independent line of argument to suggest that atropine may blur the natural input, but doesn't change the overall spontaneous activity of neurons. Further, it suggest that there is a significant physiological different in the activity distributions between unstructure input (e.g. patch) and degraded input (e.g. atropine).

In this way we may hope to constrain other parameters of the model by comparing to experimental rates of recovery.

9

References

Bienenstock, E. L., L. N Cooper, and P. W. Munro. 1982. "Theory for the Development of Neuron Selectivity: Orientation Specificity and Binocular Interaction in Visual Cortex." *Journal of Neuroscience* 2: 32–48.

Birch, Eileen E. 2013. "Amblyopia and Binocular Vision." *Progress in Retinal and Eye Research* 33: 67–84.

Blais, B. S., N. Intrator, H. Shouval, and L. N Cooper. 1998. "Receptive Field Formation in Natural Scene Environments: Comparison of Single Cell Learning Rules." *Neural Computation* 10 (7): 1797–1813.

Blais, Brian S. 1998. "The Role of the Environment in Synaptic Plasticity: towards an Understanding of Learning and Memory." PhD thesis, Brown University, Institute for Brain; Neural Systems; Dr. Leon N Cooper, Thesis Supervisor.

Blais, Brian S, Mikhail Y Frenkel, Scott R Kuindersma, Rahmat Muhammad, Harel Z Shouval, Leon N Cooper, and Mark F Bear. 2008. "Recovery from Monocular Deprivation Using Binocular Deprivation." *J Neurophysiol* 100 (4): 2217–24. https://doi.org/10.1152/jn.90411.2008.

Blais, Brian, Harel Shouval, and Leon N Cooper. 1999. "The Role of Presynaptic Activity in Monocular Deprivation: Comparison of Homosynaptic and Heterosynaptic Mechanisms." *Proc. Natl. Acad. Sci.* 96: 1083–87.

Gao, Tina Y., Cindy X. Guo, Raiju J. Babu, Joanna M. Black, William R. Bobier, Arijit Chakraborty, Shuan Dai, et al. 2018. "Effectiveness of a Binocular Video Game Vs Placebo Video Game for Improving Visual Functions in Older Children, Teenagers, and Adults with Amblyopia." *JAMA Ophthalmology* 136 (2): 172. https://doi.org/10.1001/jamaophthalmol.2017.6090.

Glaser, Stephen R, Andrea M Matazinski, David M Sclar, Nicholas A Sala, Chrissy M Vroman, Cindy E Tanner, David R Stager, et al. 2002. "A Randomized Trial of Atropine Vs Patching for Treatment of Moderate Amblyopia in Children." *Archives of Ophthalmology* 120 (3): 268–78.

Holmes, Jonathan M., Vivian M. Manh, Elizabeth L. Lazar, Roy W. Beck, Eileen E. Birch, Raymond T. Kraker, Eric R. Crouch, et al. 2016a. "Effect of a Binocular iPad Game Vs Part-Time Patching in Children Aged 5 to 12 Years with Amblyopia." *JAMA Ophthalmology* 134 (12): 1391. https://doi.org/10.1001/jamaophthalmol.2016.4262.

Holmes, Jonathan M, Vivian M Manh, Elizabeth L Lazar, Roy W Beck, Eileen E Birch, Raymond T Kraker, Eric R Crouch, et al. 2016b. "A Randomized Trial of a Binocular iPad Game Versus Part-Time Patching in Children 5 to 12 Years of Age with Amblyopia." *JAMA Ophthalmology* 134 (12): 1391.

Hubel, David H. 1995. *Eye, Brain, and Vision.* Scientific American Library/Scientific American Books.

Jeon, C J, E Strettoi, and R H Masland. 1998. "The major cell populations of the mouse retina." *J Neurosci* 18 (21): 8936–46.

Kelly, Krista R., Reed M. Jost, Lori Dao, Cynthia L. Beauchamp, Joel N. Leffler, and Eileen E. Birch. 2016. "Binocular iPad Game Vs Patching for Treatment of Amblyopia in Children." *JAMA Ophthalmology* 134 (12): 1402. https://doi.org/10.1001/jamaophthalmol.2016.4224.

Li, Simone L, Alexandre Reynaud, Robert F Hess, Yi-Zhong Wang, Reed M Jost, Sarah E Morale, Angie De La Cruz, Lori Dao, David Stager Jr, and Eileen E Birch. 2015. "Dichoptic Movie Viewing Treats Childhood Amblyopia." *J AAPOS* 19 (5): 401–5. https://doi.org/10.1016/j.jaapos.2015.08.003.

Sterling, P, M A Freed, and R G Smith. 1988. "Architecture of rod and cone circuits to the on-beta ganglion cell." *J Neurosci* 8 (2): 623–42.

Wallace, David K, Michael X Repka, Katherine A Lee, Michele Melia, Stephen P Christiansen, Christie L Morse, and Derek T Sprunger. 2018. "Amblyopia Preferred Practice Pattern®." *Ophthalmology* 125 (1): P105–42.

Wallace, DK, SA Cotter, AR Edwards, RW Beck, Pediatric Eye Disease Investigator Group, et al. 2006. "Treatment of Amblyopia with Refractive Correction Alone." *Investigative Ophthalmology & Visual Science* 47 (13): 4310–10.

Xiao, Scott, Eric D Gaier, Malcolm L Mazow, Ann U Stout, Dean A Travers, Endri Angjeli, Hank C Wu, Gil Binenbaum, and David G Hunter. 2020. "Improved Adherence and Treatment Outcomes with an Engaging, Personalized Digital Therapeutic in Amblyopia." *Scientific Reports* 10 (1): 1–8.

Zárate, Blanca Ruiz de, and Jaime Tejedor. 2007. "Current Concepts in the Management of Amblyopia." *Clinical Ophthalmology (Auckland, NZ)* 1 (4): 403.